ISBN: 978-3-95450-220-2 ISSN: 2673-5474 doi: 10.18429/JACoW-FEL2022-TUP05

RADIO-FREQUENCY-DETUNING BASED MODELING AND SIMULATION OF ELECTRON BUNCH TRAIN QUALITY

Y. Chen*
Deutsches Elektronen-Synchrotron DESY, Hamburg, Germany

Abstract

A numerical study is carried out on the quality of the electron bunch train produced from a photoinjector based on a frequency-detuning dependent gun coupler kick. The impact of the kick on the emittance of the bunch train is modelled via three-dimensional electromagnetic field maps calculated at detuned frequencies of the gun cavity within long radio-frequency pulses. Beam dynamics simulations are performed in the so-called frequency-detuning regime. Preliminary results are presented and discussed.

INTRODUCTION

Radio-Frequency (RF) photoinjectors provide high brightness electron bunches for modern linear accelerator based free-electron lasers (FEL) [1–7]. At the European XFEL [2] (EuXFEL), the photoinjector [8] consists of an L-Band RF gun, a TESLA type 1.3 GHz module (A1), a 3rd harmonic RF section (AH1), a laser heater and beam diagnostics, as shown in Fig. 1. The 1.6-cell 1.3 GHz RF gun [9] can be operated with an electric field gradient of 60 MV/m on the cathode surface with long RF pulses of up to 650 µs at 10 Hz, allowing the production of 27000 bunches per second at the EuXFEL. The RF power is provided by a 10 MW multi-beam klystron and fed to the gun from the input waveguide via a door-knob transition into the rotationally symmetric coaxial coupler and the gun cavity. A frequency-detuning dependent transient coaxial RF coupler kick is observed and characterized within the RF pulse in [10]. The impacts of the effect on the electron bunch quality along the train are more pronounced towards longer RF pulse operation of the FEL.

Since the first lasing of the EuXFEL in May 2017 [11], a growing trend in the RF pulse length of the gun has been shown for routine user experiments, i.e. from averagely 100 µs in 2017 to first-time operating with 600 µs by the end of 2019, subsequently, stably running with 500 µs and above until the present. With more pronounced frequency-detuning over longer RF macropulses, potential impacts of the above-mentioned RF coupler kick on the bunch quality along the train should be further studied.

METHODOLOGY

Experiments have shown the existence of frequency detuning of the gun cavity within the RF macropulse due to pulse heating [10]. Within the RF pulse, individual electron bunches along the train see the transverse coaxial coupler kick of the gun. The kick is varied as a function of the frequency detuning of the gun cavity. Thus, the variable kick added to different bunches along the train and the resulting impact onto the bunch quality can be modelled as these bunches passing through the gun while experiencing disturbed and detuned RF field distributions of the gun cavity. This method requires RF field calculations at detuned frequencies as well as corresponding beam dynamics simulations using these field maps, as presented in the following two sections.

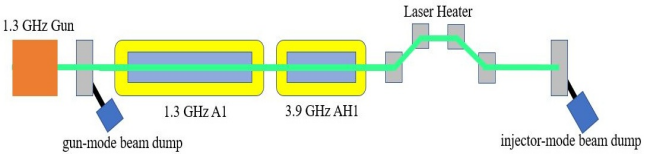

Figure 1: Schematic view of the European XFEL photoinjector (not to scale).

ELECTROMAGNETIC FIELDS

The three-dimensional calculation of the disturbed RF cavity field due to the gun coupler kick is based on the frequency domain solver of Computer Simulation Technology [12]. A computational model with its coordinate system is described in [10]. The frequency detuning (Δf) is defined as the difference between the RF drive frequency (f) and the cavity resonance frequency (f_0), i.e. $\Delta f = f - f_0$. In the following example, the S11 parameter, defined as the ratio of the reflected power over the forward power for a resonant cavity, is tuned to about -25 dB at the resonance. Figure 2 shows the disturbed transverse electric (Ey) and magnetic (Hx) field profiles at different detuned frequencies of the gun cavity, covering a detuning range up to +15 kHz towards a deeper over-heating state of the gun.

SIMULATIONS

Beam dynamics simulations are performed using ASTRA [13]. A simulation setup is sketched in Fig. 1. Electron bunches are tracked with on-crest RF phasing until the exit of the A1 module. The final beam energy is 150 MeV. Note, in addition, that a three-dimensional TESLA cavity field map of the A1 module is also applied [14, 15].

Figure 3 shows a comparison of the projected transverse emittance evolution along the beamline between two simulation cases. One of the cases (blue curve) serves as a reference, in which, under ideal conditions, no coupler kick effects are considered. In the other case (orange curve), a specific situation is emulated: a bunch travels through the gun and the A1 module both of which are described by the

* ye.lining.chen@desy.de

ISBN: 978-3-95450-220-2 ISSN: 2673-5474 doi: 10.18429/JACoW-FEL2022-TUP05

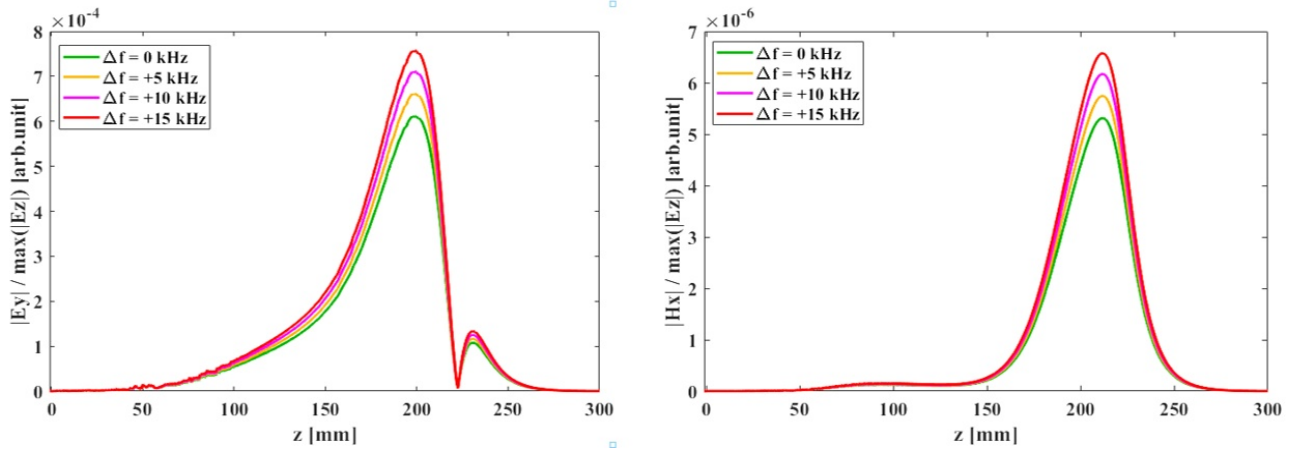

Figure 2: Disturbed RF field distributions with the normalized amplitudes to the accelerating fields at detuned resonance frequencies of the gun cavity. Left: electric fields; right: magnetic fields.

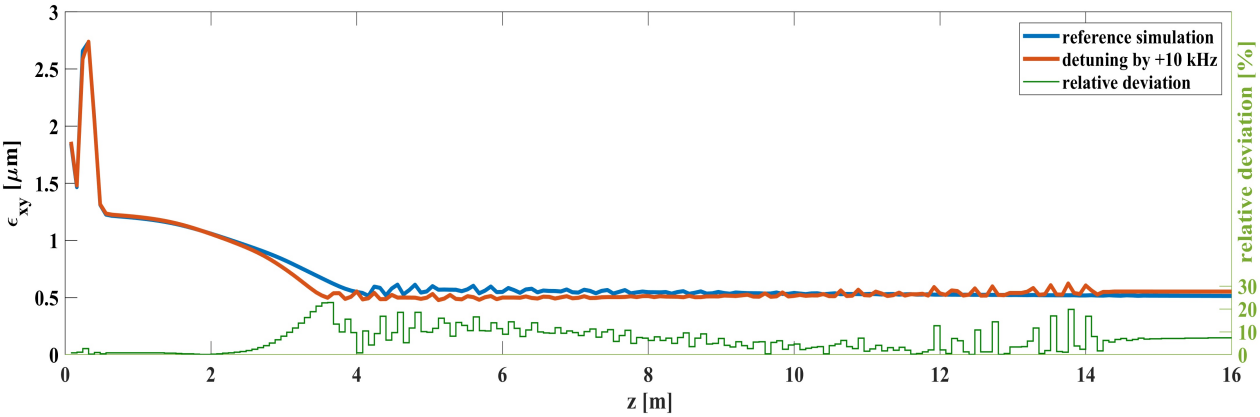

Figure 3: A comparison of the projected transverse emittance along the beamline between a reference simulation (no coupler kicks) and a simulation performed at 10 kHz off-resonance of the gun cavity. The final emittance is calculated at the exit of the A1 module, i.e. about 16 m downstream the cathode, as shown in Fig. 1.

corresponding three-dimensional field maps. Particularly for the gun field map, a 10 kHz frequency detuning is assumed. As an empirical estimation, a simulated 10-kHz detuning of the gun cavity may correspond to about 30 kW power reflection when the gun is practically operated at about 5.4 MW. Other simulation settings are kept the same in both cases. The relative difference in emittance (green curve) is illustrated on the right axis. As a result, for an electron bunch sitting on an intra-RF-pulse location of 10 kHz off the gun resonance, its projected transverse emittance grows by about 7% with respect to an ideal coupler-kick-free case.

Figure 4 shows a relative emittance change as a function of frequency detuning of the gun cavity. The gun solenoid strength is fixed and not explicitly optimized for a smaller transverse emittance at any reference point. In this figure, different detuned frequencies correspond to different locations within the RF macropulse (towards an over-heated state w.r.t. the gun resonance), thereby representing the cases of different electron bunches along the train. This numerical example shows an overall emittance deviation along the bunch train (reflected by the frequency detuning) downstream the A1 module. More specifically, within a 10-kHz detuning of the gun cavity over the RF macropulse, seen by the electron bunch train, the projected emittance change is up to about 22%. It can also be noted that higher frequency detuning towards a deeper over-heated state of the gun is generally more beneficial for the emittance reduction.

A parametric dependency of the effect on the gun solenoid strength is shown in Fig. 5. At a fixed detuned frequency of the gun cavity, it is obvious that the overall emittance at the exit of the A1 module depends on the strength of the gun solenoid. However, at each detuned frequencies of the gun cavity, an optimal gun solenoid strength for achieving an overall optimized transverse emittance after the A1 module may not be the same. This also indicates that the peak to peak variation of the projected transverse emittance along the bunch train may have a parametric dependency on the chosen solenoid strength. These interrelated parametric dependencies (e.g. on RF phases, solenoid strength, orbit at the entrance of the A1 module, etc.) needs to be further clarified.

ISBN: 978-3-95450-220-2 ISSN: 2673-5474 doi: 10.18429/JACoW-FEL2022-TUP05

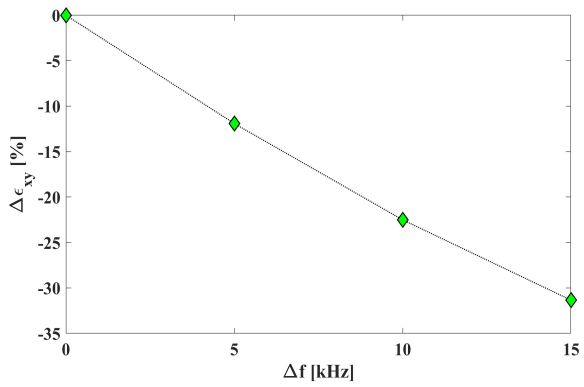

Figure 4: Relative emittance change versus frequency detuning within the RF pulse of the gun cavity. The emittance is calculated at the exit of the A1 module. The gun solenoid strength is fixed.

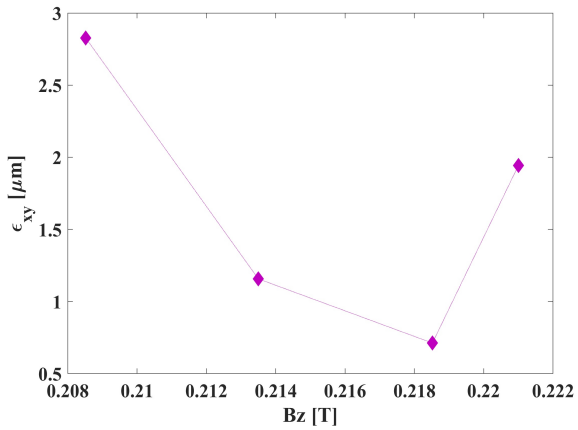

Figure 5: Gun solenoid strength dependency of an optimized projected emittance at a fixed detuned frequency of the gun cavity using on-crest phasing of both the gun and the A1 module.

OUTLOOK

Numerical studies presented in this paper suggest a relative projected transverse emittance change up to 22% along an electron bunch train contained within an RF macropulse of the gun cavity over a frequency detuning of 10 kHz with respect to the resonance. More detailed investigations will be focused on a comparison of the bunch quality with the measurement data, as well as potential impacts onto the FEL performance.

ACKNOWLEDGEMENTS

The author acknowledges support from Deutsches Elektronen-Synchrotron DESY (Hamburg, Germany), a member of the Helmholtz Association HGF and European XFEL GmbH (Schenefeld, Germany). The author thanks Martin Dohlus from DESY for useful discussions on coupler kicks of TESLA cavities and for providing helpful references.

REFERENCES

[1] M. Dohlus *et al.*, "Synchrotron Radiation and Free-Electron Lasers". In *Landolt-Boernstein New Series*; Myers, S., Schopper, H., Eds.; Springer: Berlin/Heidelberg, Germany, 2013; Volume 21C. doi:10.1007/978-3-642-23053-0$_$41

[2] W. Decking *et al.*, "A MHz-repetition-rate hard X-ray free-electron laser driven by a superconducting linear accelerator", *Nat. Photonics*, vol. 14, pp.391–397, 2020. doi:10.1038/s41566-020-0607-z

[3] E. Prat *et al.*, "A compact and cost-effective hard X-ray free-electron laser driven by a high-brightness and low-energy electron beam", *Nat. Photonics*, vol. 14, pp. 748–754, 2020. doi:10.1038/s41566-020-00712-8

[4] P. Emma *et al.*, "First lasing and operation of an ångstrom-wavelength free-electron laser", *Nat. Photonics*, vol. 2010, vol. 4, p. 641–647. doi:10.1038/nphoton.2010.176

[5] T. Ishikawa *et al.*, "A compact X-ray free-electron laser emitting in the sub-ångström region", *Nat. Photonics*, vol. 6, pp. 540–544, 2012. doi:10.1038/nphoton.2012.141

[6] H. Kang *et al.*, "Hard X-ray free-electron laser with femtosecond-scale timing jitter", *Nat. Photonics*, vol. 11, pp. 708–713, 2017. doi:10.1038/s41566-017-0029-8

[7] A. Novokhatski, F.-J. Decker, Y. Nosochkov, and M. K. Sullivan, "The Effect of Wakefields on the FEL Performance", in *Proc. FEL'15*, Daejeon, Korea, Aug. 2015, pp. 161–165. doi:10.18429/JACoW-FEL2015-MOP055

[8] F. Brinker, "Commissioning of the European XFEL Injector", in *Proc. IPAC'16*, Busan, Korea, May 2016, pp. 1044–1047. doi:10.18429/JACoW-IPAC2016-TUOCA03

[9] M. Krasilnikov *et al.*, "Experimentally minimized beam emittance from an L-band photoinjector", *Phys. Rev. Accel. Beams*, vol. 15, p. 100701, 2012. doi:10.1103/PhysRevSTAB.15.100701

[10] Y. Chen *et al.*, "Frequency-detuning dependent transient coaxial rf coupler kick in an *L*-band long-pulse high-gradient rf photogun", *Phys. Rev. Accel. Beams*, vol. 23, p. 010101, 2020. doi:10.1103/PhysRevAccelBeams.23.010101

[11] H. Weise and W. Decking, "Commissioning and First Lasing of the European XFEL", in *Proc. FEL'17*, Santa Fe, NM, USA, Aug. 2017, pp. 9–13. doi:10.18429/JACoW-FEL2017-MOC03

[12] Computer Simulation Technology. https://www.3ds.com/.

[13] A Space Charge Tracking Algorithm. https://www.desy.de/~mpyflo/.

[14] P. Piot, M. Dohlus, K. Floettmann, M. Marx, and S. G. Wipf, "Steering and Focusing Effects in TESLA Cavity Due to High Order Mode and Input Couplers", in *Proc. PAC'05*, Knoxville, TN, USA, May 2005, paper WPAT083, pp. 4135–4137.

[15] 3D TESLA cavity field maps. https://www.desy.de/fel-beam/s2e/codes.html.